

MODELING BUBBLE GROWTH IN MICRO-CHANNEL COOLING SYSTEMS

MIDN 1/C J. L. NICKERSON

2006-2007

---

JOSH L. NICKERSON, MIDN, USN

---

ASSOCIATE PROFESSOR SONIA M. GARCIA, MATHEMATICS

---

PROFESSOR MARTIN CERZA, MECHANICAL ENGINEERING

---

PROFESSOR THOMAS J. SANDERS, CHAIR, MATHEMATICS DEPT.

# MODELING BUBBLE GROWTH IN MICRO-CHANNEL COOLING SYSTEMS

## ABSTRACT

The project goal is to develop a mathematical model for bubble growth in a micro-channel cooling system. The problem of heat transfer from high performance microprocessors is introduced. Equations for volumetric bubble growth rate and local heat transfer coefficients shown to depend on the temperature profile beneath the bubble's base. The three-dimensional problem is simplified to a two-dimensional cross-section along the micro-channel. A partial differential equation is then solved resulting in a function for the temperature profile. The equation for local heat transfer coefficient is solved. These solutions are incorporated into a MatLab program for analysis. Plots of temperature profile and local heat transfer coefficients are generated.

## INTRODUCTION

Microprocessors are a widespread and important component of modern computing devices. The heat generated by a processor increases with the number of operations per second. This heat must be carried away somehow to prevent the processor components from melting. Conventional devices employ simple air-convection fans to achieve this cooling effect. However, such a cooling mechanism has limits, which current processor designs may be approaching. In particular, the U.S. Navy's Office of Naval Research has set a target heat flux of 1 kW/cm<sup>2</sup> for processors in an advanced RADAR system, and that amount of heat simply cannot be driven away using a conventional cooling system. An alternative to cooling via air convection is the use of micro-channels embedded in the microprocessor. Coolant flows through the channels, carrying heat away from the processor components. The physical mechanism for this cooling effect is latent heat. Heat flux from the processor results in the formation of bubbles in the micro-channel. Though some physical experimentation has taken place, very little mathematical modeling has been done regarding formation and growth of bubbles in micro-channels. The goal of this research project is to develop a mathematical model for bubble growth in a micro-channel cooling system.

## MATHEMATICAL SOLUTIONS

The model for bubble growth rate by volume will be obtained using the following relationship (see Appendix 1 for explanation of parameters):

$$\rho_g h_{fg} \frac{\partial (Vol)}{\partial t} = kA \left( \frac{\partial T}{\partial y} \right)_{y=0} \quad (1)$$

The formula for the local heat transfer coefficient is provided by the following:

$$h = \frac{k \left( \frac{\partial T}{\partial y} \right)_{y=0}}{T_{wall} - T_{sat}} \quad (2)$$

It is noted that both of these equations are dependent on the term  $T$  which represents the temperature profile under the bubble base. Before proceeding further with development of the mathematical model, then, a solution for this temperature profile must be obtained.

The following figure represents the three-dimensional situation of a single bubble within a micro-channel:

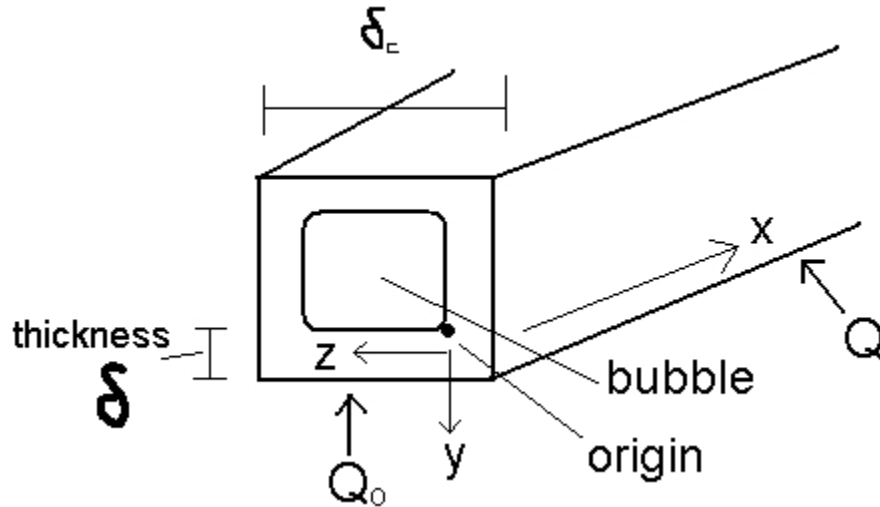


Figure 1: 3-D representation of single bubble in channel

The  $x, y, z$  coordinate system is indicated on the figure.  $Q$  represents incoming heat flux from the processor. The parameter  $\delta$  represents the thickness of the liquid layer beneath the bubble, while  $\delta_c$  represents the width of the micro-channel. Because  $\delta$  is very small compared to  $\delta_c$ , the above can be simplified to a two-dimensional cross-section by ignoring the  $z$  coordinate:

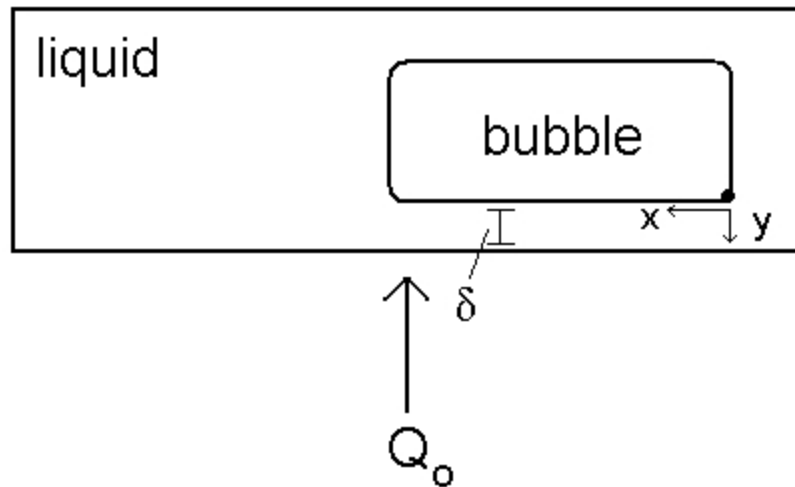


Figure 2: 2-D cross-section of single bubble in channel, ignoring  $z$

The origin for the coordinate system is set at the leading edge of the bubble, to the right on Figure 2. Though the bubble is moving down the channel and growing, the origin remains fixed at this leading edge.

The situation in Figure 2 is represented in the following partial differential equation:

$$\frac{\partial^2 T}{\partial y^2} = f(y) \cdot \frac{\partial T}{\partial x} \quad (3)$$

Where  $f(y)$  represents the fluid velocity profile under the bubble. Further simplifying, it is assumed that  $f(y) = u_{avg}$  where  $u_{avg}$  is the average velocity of the liquid beneath the bubble. The resulting partial differential equation, which must be solved for the temperature profile in the liquid layer beneath the bubble base, then becomes:

$$\frac{\partial^2 T}{\partial y^2} = \frac{u_{avg}}{\alpha} \cdot \frac{\partial T}{\partial x} \quad (4)$$

Because  $y$  ranges from 0 to  $\delta$  and  $\delta$  is very small compared to  $x$  (distance down the channel), the effects of any non-linear terms in the function for the temperature profile may not be evident except at extremely small values for  $x$ . For this reason, it is necessary to non-dimensionalize  $x$  and  $y$  via the following:

$$\text{Let } x^* = \frac{x}{\delta} \text{ and let } y^* = \frac{y}{\delta}$$

The resulting non-dimensionalized partial differential equation is

$$\frac{\partial^2 T}{\partial y^{*2}} = \frac{\delta \cdot u_{avg}}{\alpha} \cdot \frac{\partial T}{\partial x^*} \quad (5)$$

The equation is subject to the following conditions:

- (i)  $T(x^*, 0) = T_{sat}$
- (ii)  $T(0, y^*) = T_{mf}$
- (iii)  $\frac{\partial T}{\partial y^*}(x^*, 1) = \frac{Q_0 \delta}{k}$

The analytical solution of (5) begins with a transformation to a homogeneous boundary condition:

$$\text{Let } \theta = T(x, y) - T_{sat}$$

$$\text{Then } \partial \theta = \partial T$$

The resulting partial differential equation is then:

$$\frac{\partial^2 \theta}{\partial y^{*2}} = \frac{\delta \cdot u_{avg}}{\alpha} \cdot \frac{\partial \theta}{\partial x^*} \quad (6)$$

and is subject to:

- (i)  $\theta(x^*, 0) = 0$
- (ii)  $\theta(0, y^*) = T_{mf} - T_{sat}$

$$(iii) \frac{\partial \theta}{\partial y^i}(x^i, 1) = \frac{Q_0 \delta}{k}$$

Next, the function  $\theta$  is split up into two functions, one function in both x and y and one function in y only:

$$\text{Let } \theta(x^i, y^i) = \psi(x^i, y^i) + \varphi(y^i)$$

Performing this substitution results in the following equation:

$$\frac{\partial^2 \psi}{\partial y^{i2}} + \frac{\partial^2 \varphi}{\partial y^{i2}} = \frac{\delta \cdot u_{avg}}{\alpha} \cdot \frac{\partial \psi}{\partial x^i} \quad (7)$$

which is subject to:

$$\begin{aligned} (i) & \psi(x^i, 0) + \varphi(0) = 0 \\ (ii) & \psi(0, y^i) + \varphi(y^i) = T_{mf} - T_{sat} \\ (iii) & \frac{\partial \psi}{\partial y^i}(x^i, 1) + \frac{\partial \varphi}{\partial y^i}(1) = \frac{Q_0 \delta}{k} \end{aligned}$$

This partial differential equation and its conditions are then split into the following:

$$\begin{aligned} (1) \quad & \frac{d^2 \varphi}{dy^{i2}} = 0 \quad \text{subject to} \quad (i) \quad \varphi(0) = 0 \\ & (ii) \quad \frac{d\varphi}{dy^i}(1) = \frac{Q_0 \delta}{k} \\ (2) \quad & \frac{\partial^2 \psi}{\partial y^{i2}} = \frac{\delta \cdot u_{avg}}{\alpha} \cdot \frac{\partial \psi}{\partial x^i} \quad \text{subject to} \quad (i) \quad \psi(x^i, 0) = 0 \\ & (ii) \quad \psi(0, y^i) = T_{mf} - T_{sat} - \frac{Q_0 \delta}{k} \cdot y^i \\ & (iii) \quad \frac{\partial \psi}{\partial y^i}(x^i, 1) = 0 \end{aligned}$$

The first part is an ordinary differential equation which is easily solved for

$$\varphi(y^i) = \frac{Q_0 \delta}{k} \cdot y^i$$

The second part is solved analytically via separation of variables:

$$\begin{aligned}
\psi(x^i, y^i) &= X(x^i) \cdot Y(y^i) \\
\Rightarrow X'Y &= \frac{\alpha}{\delta \cdot u_{avg}} \cdot XY'' \\
\Rightarrow \frac{X'}{\left(\frac{\alpha}{\delta \cdot u_{avg}}\right)X} &= \frac{Y''}{Y} = -\lambda_n^2
\end{aligned}$$

Because X and Y are functions of independent variables, their ratios above must be equal to some constant which is denoted  $-\lambda_n^2$  here. The above is divided into two problems, one solved for the function X and the other solved for the function Y. The result of applying separation of variables is the following:

$$\begin{aligned}
X(x^i) &= A_n e^{-\lambda_n^2 \left(\frac{\alpha}{\delta \cdot u_{avg}}\right) x^i} \quad \text{and} \\
Y(y^i) &= c_1 \sin(\lambda_n y^i) + c_2 \cos(\lambda_n y^i) \\
\Rightarrow \psi(x^i, y^i) &= A_n e^{-\lambda_n^2 \left(\frac{\alpha}{\delta \cdot u_{avg}}\right) x^i} \left[ c_1 \sin(\lambda_n y^i) + c_2 \cos(\lambda_n y^i) \right]
\end{aligned}$$

Using condition (7)(i) it is determined that  $c_2 = 0$  and therefore

$$\begin{aligned}
\psi(x^i, y^i) &= \sum_{n=1}^{\infty} A_n e^{-\lambda_n^2 \left(\frac{\alpha}{\delta \cdot u_{avg}}\right) x^i} \sin(\lambda_n y^i) \\
\text{and } \varphi(y^i) &= \frac{Q_0 \delta}{k} \cdot y^i
\end{aligned}$$

Having solved for  $\psi$  and  $\varphi$ , back-substitution provides the solution for  $\theta$ ; one further step yields the function  $T$  for the temperature profile beneath the bubble base.

$$\begin{aligned}
\theta(x^i, y^i) &= \psi(x^i, y^i) + \varphi(y^i) \\
\Rightarrow \theta(x^i, y^i) &= \left[ \sum_{n=1}^{\infty} A_n e^{-\lambda_n^2 \left(\frac{\alpha}{\delta \cdot u_{avg}}\right) x^i} \sin(\lambda_n y^i) \right] + \frac{Q_0 \delta}{k} \cdot y^i \\
\theta = T(x^i, y^i) - T_{sat} &\Rightarrow T(x^i, y^i) = \theta(x^i, y^i) + T_{sat} \\
\Rightarrow T(x^i, y^i) &= \left[ \sum_{n=1}^{\infty} A_n e^{-\lambda_n^2 \left(\frac{\alpha}{\delta \cdot u_{avg}}\right) x^i} \sin(\lambda_n y^i) \right] + \frac{Q_0 \delta}{k} \cdot y^i + T_{sat}
\end{aligned}$$

Employing condition (7)(ii) it is possible to solve for the formula for the Fourier coefficients,  $A_n$ . The resulting formula for Fourier coefficients is

$$A_n = 2 \int_0^1 \left( T_{mf} - T_{sat} - \frac{Q_0 \delta}{k} \cdot y^i \right) \sin(\lambda_n y^i) dy^i$$

This rather complicated formula can be easily simplified through the following substitution:

$$\text{Let } \theta_{\text{sup}} = T_{\text{sup}} - T_{\text{sat}} \text{ where } T_{\text{sup}} = T_{mf} - \frac{Q_0 \delta}{k} \cdot y^i$$

$$\Rightarrow A_n = 2\theta_{\text{sup}} \int_0^1 \sin(\lambda_n y^i) dy^i = \frac{2\theta_{\text{sup}}}{\lambda_n}$$

Condition (7)(iii) is used to solve for the eigenvalues,  $\lambda_n$ . The resulting formula for the eigenvalues is

$$\lambda_n = \frac{(2n-1) \cdot \pi}{2}$$

The final solution for the temperature profile under the bubble base is then

$$T(x^i, y^i) = \left[ \sum_{n=1}^{\infty} A_n e^{-\lambda_n^2 \left( \frac{\alpha}{\delta \cdot u_{\text{avg}}} \right) \cdot x^i} \sin(\lambda_n y^i) \right] + \frac{Q_0 \delta}{k} \cdot y^i + T_{\text{sat}}$$

where

$$A_n = \frac{2\theta_{\text{sup}}}{\lambda_n} \quad \lambda_n = \frac{(2n-1) \cdot \pi}{2}$$

And all other parameters are constants, with the obvious exceptions of  $x^i$  and  $y^i$ .

Having obtained  $T$ , it is necessary to calculate  $\left( \frac{\partial T}{\partial y} \right)_{y=0}$  to solve for the local heat transfer coefficient. Differentiating the above with respect to  $y^i$  and evaluating at  $y^i = 0$  results in

$$\left( \frac{\partial T}{\partial y^i} \right)_{y=0} = \left[ \sum_{n=1}^{\infty} A_n \lambda_n e^{-\lambda_n^2 \left( \frac{\alpha}{\delta \cdot u_{\text{avg}}} \right) \cdot x^i} \right] + \frac{Q_0 \delta}{k}$$

Finally, this result is substituted into (2), providing a solution for local heat transfer coefficient  $h$  as a function of  $x^i$ .

## DISCUSSION AND RESULTS

With the solutions for temperature profile and local heat transfer coefficient obtained, a MatLab program can be developed incorporating them. MatLab is then used to generate data in the form of plots. These plots are used to verify that the solutions obtained thus far are valid, and thus may be used in the bubble growth model. Data from these solutions can also be compared to experimental data for further validation of the model. For the plots below, the coolant is assumed to be water.

The first plot generated represents level curves of the temperature profile, depicting curves of temperature vs.  $y$  at unique  $x$  values.

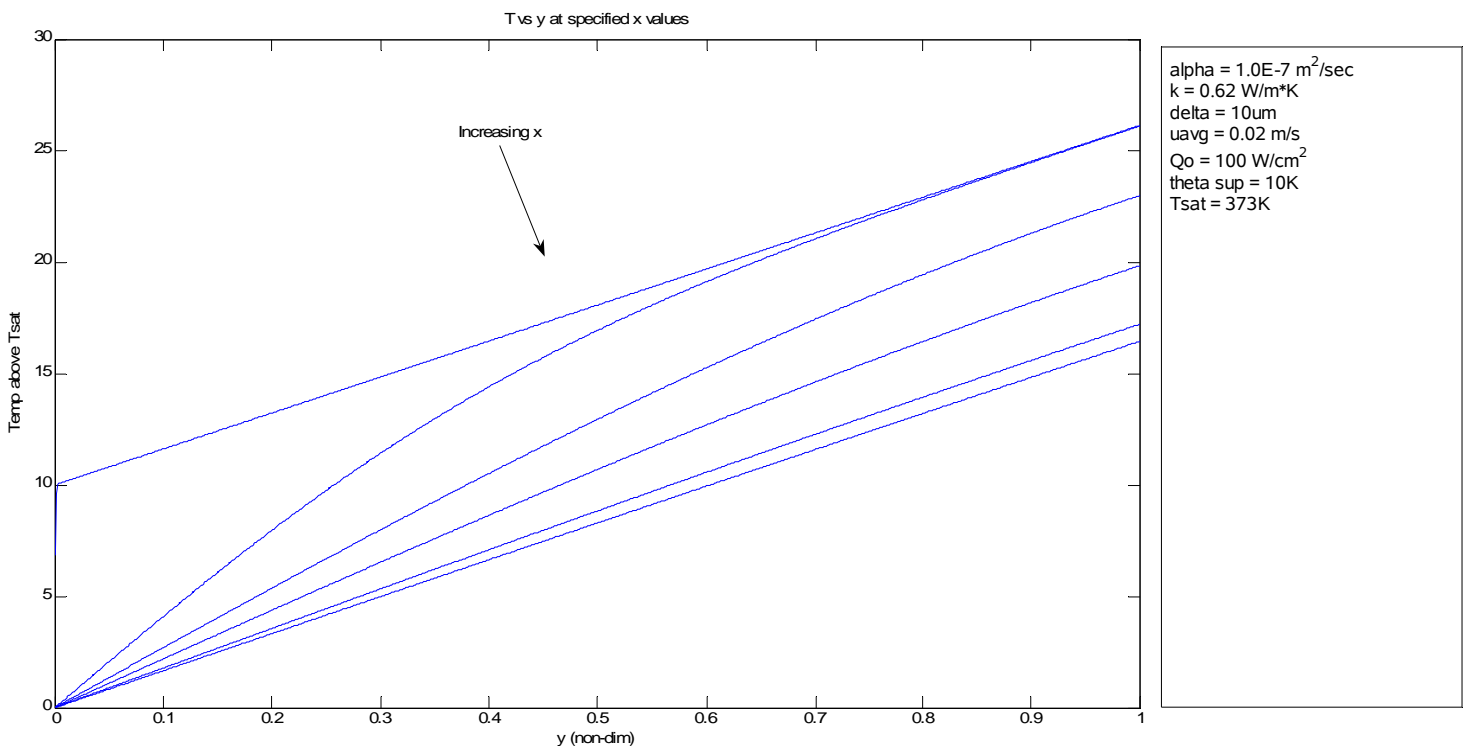


Figure 3: Plot of  $T(x,y)$  vs.  $y$  at unique  $x$  values

It should be noted that  $y=0$  corresponds to the base of the bubble, while  $y=1$  corresponds to the micro-channel wall. The  $x$  variable starts at 0 and increases through values of 0.1, 0.5, 1, 2, and 3. Values beyond that are very difficult to distinguish from the line at  $x=3$ , the lowest line on the plot. The effect of the non-linear terms in the function for  $T(x,y)$  is noticeable in the level curves. As  $x$  increases, the exponential term dies out, and the linear term dominates.

Because  $T$  is a function of  $x$  and  $y$ , the temperature profile may be better represented by a three-dimensional surface plot, which allows viewing of all possible values for a given set of parameters simultaneously.

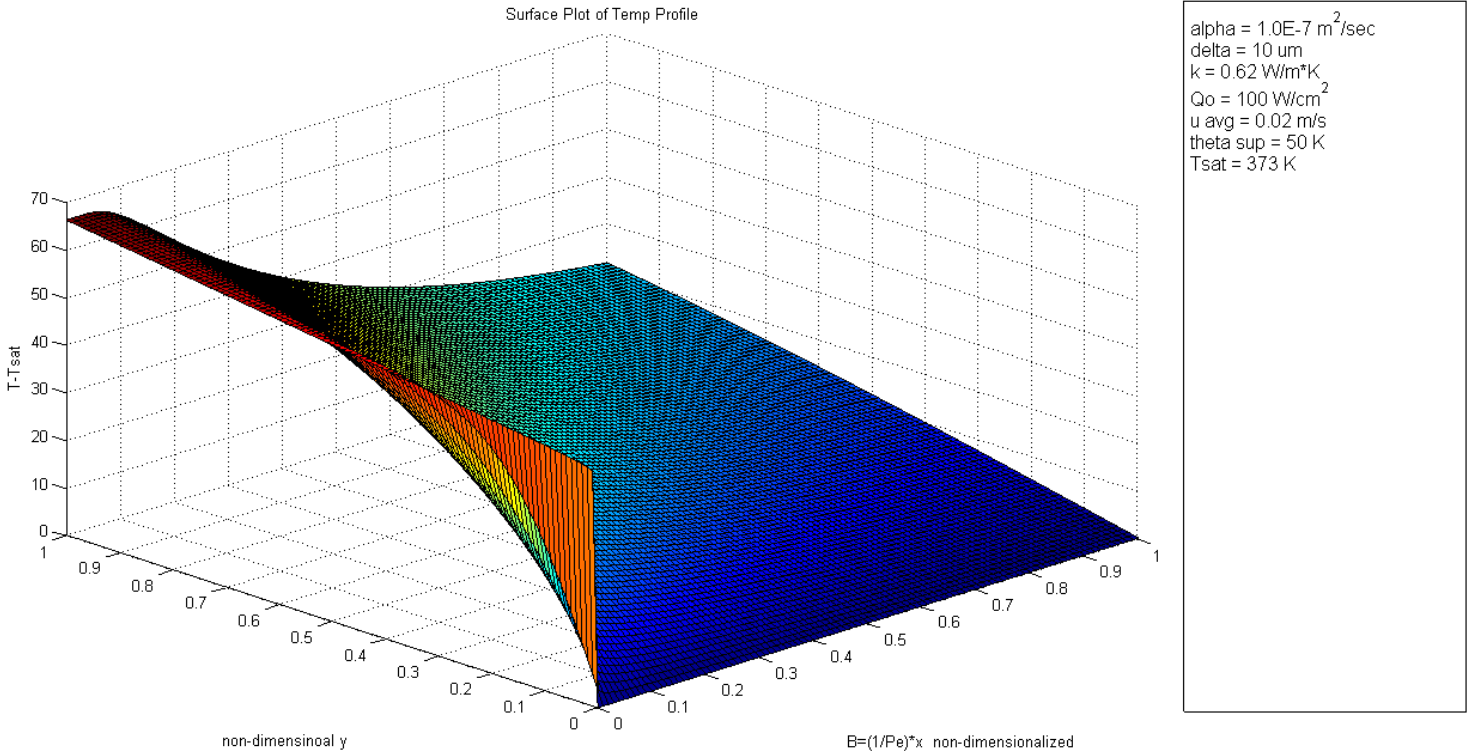


Figure 4: Surface plot of temperature profile at  $\theta_{sup} = 50$  Kelvin

In this plot, rather than displaying  $T$  vs.  $x$  and  $y$ ,  $T$  was plotted against  $y$  and a grouping “ $B$ ” where

$$B = \frac{\alpha \cdot x^2}{\delta \cdot u_{avg}}$$

which better incorporates into the plot the effects of other parameters. From this surface plot it is readily apparent that as distance down the channel increases, the nonlinear terms in  $T$  tend towards zero and the surface becomes more planar. The origin of the level curves from Figure 3 is also apparent as the surface curvature is higher for small values of  $B$ . Similar plots were generated for values of  $\theta_{\text{sup}} = 10$  Kelvin and  $\theta_{\text{sup}} = 100$  Kelvin, shown below.

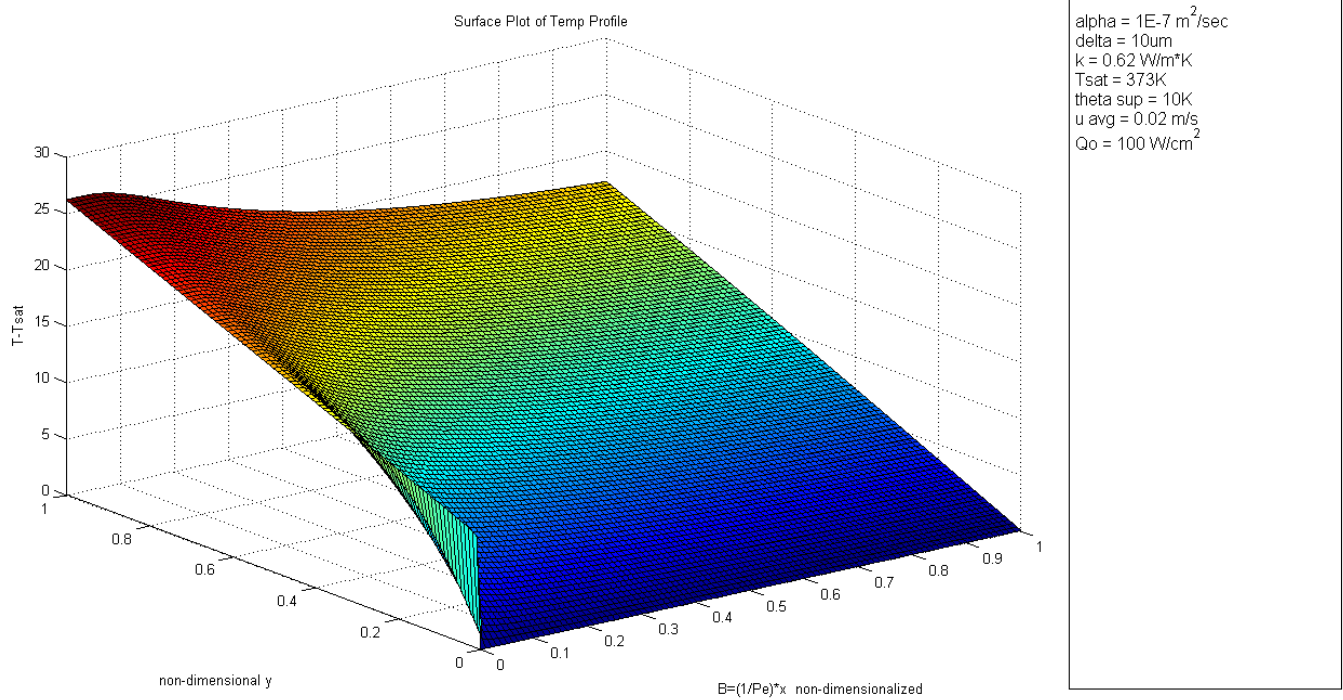


Figure 5: Surface plot of temperature profile at  $\theta_{\text{sup}} = 10$  Kelvin

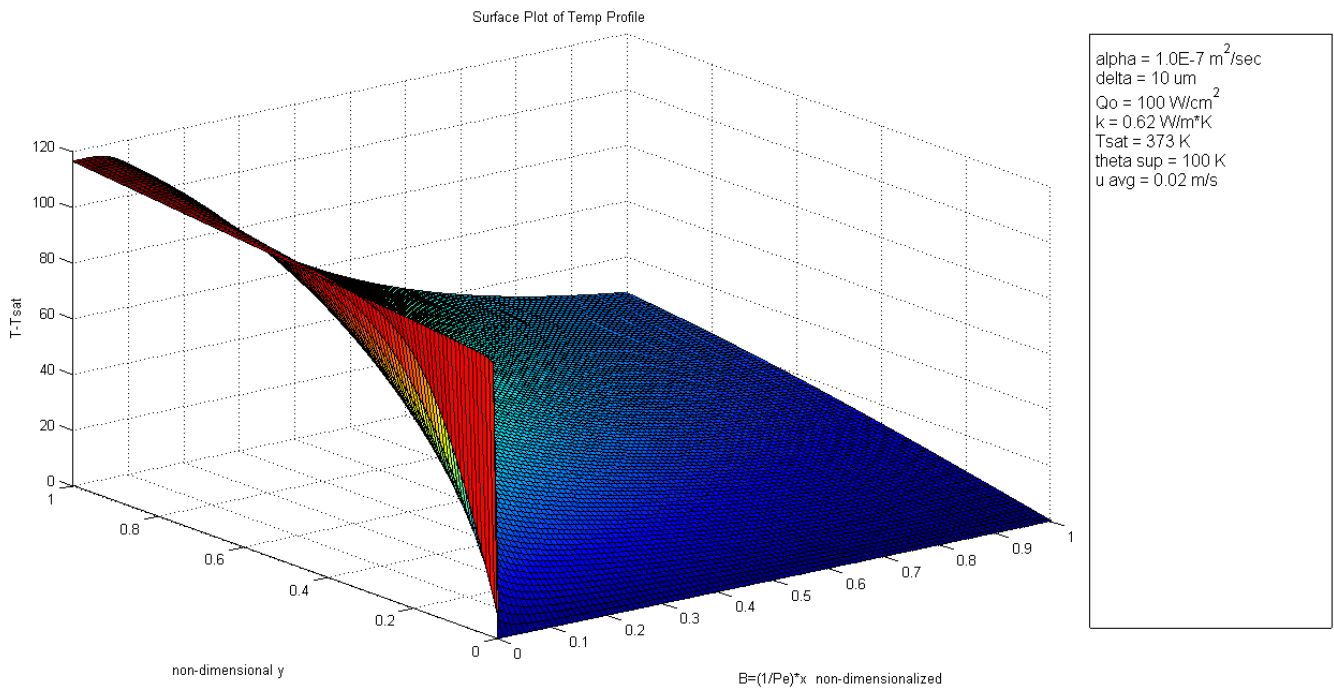


Figure 6: Surface plot of temperature profile at  $\theta_{\text{sup}} = 100$  Kelvin

Decreasing  $\theta_{\text{sup}}$  to 10 Kelvins results in a lower initial temperature on the surface plot, and the surface appears more planar. Likewise, increasing  $\theta_{\text{sup}}$  to 100 Kelvins has the opposite effect, raising the initial temperature and prolonging the curvature of the surface a greater distance down the micro-channel.

Local heat transfer coefficients vary with  $x$ , and should approach a steady-state value with increasing distance down the channel. Plots of  $h$  vs.  $x$  should illustrate this relationship. The following figure displays several plots of  $h$  vs.  $x$  at varying values of  $\theta_{\text{sup}}$ .

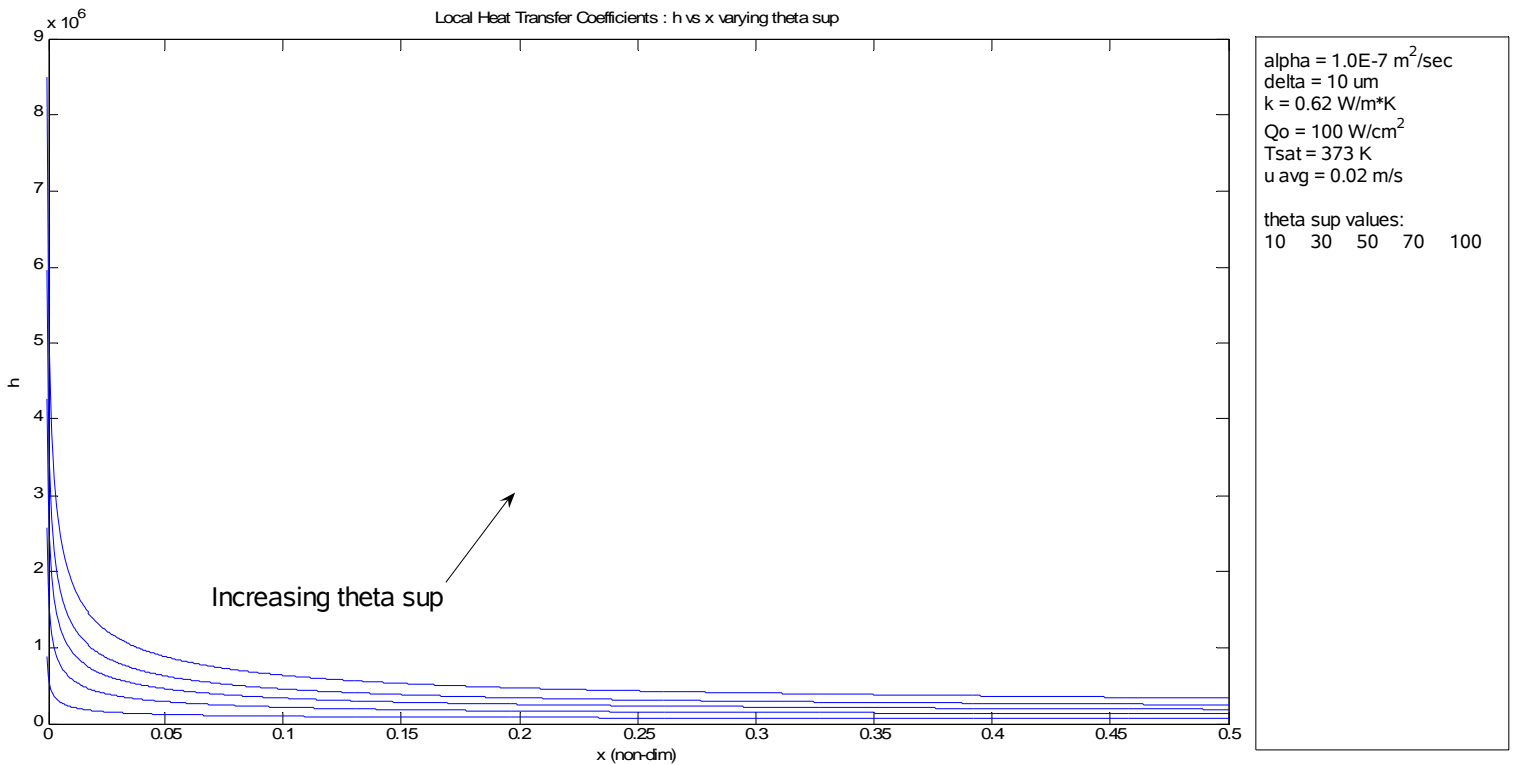


Figure 7: Plots of  $h$  vs.  $x$  at increasing values of  $\theta_{sup}$

The behavior of the plots is as expected; each settles to a steady-state value fairly quickly. With increasing  $\theta_{sup}$ , the curve shifts upward and reaches its steady-state value more slowly.

## CONCLUSIONS

The solutions obtained for the temperature profile in the liquid layer under the bubble base, as well as for the local heat transfer coefficients, appear to be valid and could therefore be incorporated into the bubble growth model as the project continues. Both level curve and surface plot representations of the temperature profile behave as expected based on physical parameters, validating the model as developed up to this point. Similarly, plots of local heat transfer coefficient versus channel length behave as expected. With increasing distance down the micro-channel, local heat transfer coefficients decrease and approach a steady-state value. With increasing  $\theta_{sup}$ , the steady-state value is increased and achieved at greater distance down the channel.

Decreasing  $\theta_{\text{sup}}$  lowers temperatures throughout the temperature profile and results in a more planar temperature profile surface. Increasing  $\theta_{\text{sup}}$  shifts the surface upwards to higher temperatures and results in greater curvature.

There are several goals for the project continuing into the Spring 2007 semester. So far, only water has been considered as a coolant, but it is possible that other coolants could be more desirable. One example is FC-72. The existing model is capable of generating similar data and plots by adjusting the parameters to the properties of the alternative coolant. Another objective is to solve equation (1) for the bubble growth rate by volume, which constitutes the actual bubble growth model. In addition, obtaining experimental data and comparing it to data from the mathematical model is a key element in validating the model. If data from an outside source can be obtained next semester, this comparison will be done.

Other, more peripheral goals for next semester include analyzing the effect of the bubble in an increasing superheated channel, analyzing the bubble at zero velocity, and mathematical modeling of annular films.

## APPENDIX 1: EXPLANATION OF PARAMETERS

A large number of variables and constants appeared throughout the solution for the temperature profile and local heat transfer coefficients; each is defined here.

$\alpha$	Thermal diffusivity of coolant $\left(\frac{m^2}{sec}\right)$ ; $\alpha = \frac{k}{c\rho}$ where $k =$ thermal conductivity $c =$ thermal capacity $\rho =$ density
$\delta$	Thickness of liquid film layer beneath bubble base; 10 $\mu$ m in examples above
$\delta_c$	Width of micro-channel
$\lambda_n$	Eigenvalues; see page 7
$\theta_{sup}$	Constant equal to $T_{sup} - T_{sat}$
$A_n$	Fourier coefficients; see page 7
$h$	Local heat transfer coefficient; see page 2 equation (2)
$k$	Thermal conductivity $\left(\frac{W}{m \cdot K}\right)$
$Q_0$	Incoming heat flux from processor $\left(\frac{W}{m^2}\right)$
$T$	Function for temperature profile in liquid layer under bubble base, a function of x, y, and z. Output in Kelvins.
$T_{mf}$	Mean fluid temperature of liquid layer at bubble's leading edge
$T_{sat}$	Coolant saturation temperature (373K for water)
$T_{sup}$	Temperature outside the bubble at a point just outside at the origin
$T_{wall}$	Temperature at channel wall, $y = \delta$ ( $y^* = 1$ )
$u_{avg}$	Average velocity of liquid beneath the bubble
$x$	Coordinate of distance along micro-channel
$y$	Coordinate of distance from bubble into liquid layer beneath bubble base
$z$	Coordinate of distance from bubble's leading edge across width of channel; ignored in two-dimensional simplification

## REFERENCES

- Farlow, S.J. Partial Differential Equations for Scientists and Engineers. Hoboken, NJ: John Wiley & Sons Inc., 1982.
- Thomas, Lindon C. Heat Transfer. Englewood Cliffs, NJ: Prentice Hall Inc., 1992.
- MATLAB version 7.0.1.15. Natick, MA: The MathWorks Inc., 2004.
- Cerza, Martin and V. Sernas. "A bubble growth model for nucleate boiling in thin, falling, superheated, laminar, water films." International Journal of Heat and Mass Transfer 28 (1985): 1307-1316.